



Research Article

Comparison on mechanical properties, damage evolution and aging effects of multi-delaminated composites under three point bending

Reng Qin^{1,2} · Wei Zhou^{1,2}  · Kang-ning Han^{1,2} · Yan-jing Zhang^{1,2} · Lian-hua Ma^{1,2}

Received: 16 March 2020 / Accepted: 24 August 2020 / Published online: 31 August 2020
© Springer Nature Switzerland AG 2020

Abstract

The study on natural aging of fiber reinforced composite, delamination damage behavior and damage pattern recognition plays a significant role in structural health monitoring of the material. In this study, acoustic emission is used to investigate damage evolution process and damage mechanisms in unidirectional glass and carbon-glass orthogonal woven fiber reinforced composites containing symmetric multiple delaminations under three point bending testing. Based on the principle of control variables, four kinds of specimens are manufactured to investigate the comparative study for the effects of delaminations, reinforced materials and fiber orientation on buckling failure behaviors and the effects of aging on mechanical properties. The results indicate that the degradation of strength and stiffness of composite can be influenced by the existence of delamination defects and natural aging condition. Both negative and positive effects can be generated by natural aging condition. Moreover, reinforced materials, porosity and fiber orientation are important factors influencing the reliability of composite. Clustering results of unidirectional fiber reinforced composites indicate interphase failure is the main damage component, moreover, the existence of symmetrical multiple delaminations will aggravate the damage of composite and make instability failure characterized by intermittency.

Keywords Delamination · Acoustic emission · Mechanical property · Damage mechanism · Natural aging effect

1 Introduction

Fiber reinforced polymer (FRP) composite has gained its reputation in the fields of automobile, aerospace and sports due to a series of good mechanical properties such as high specific strength and specific modulus, good design-ability and resistance to dynamic fatigue [1–3]. However, a lot of damages such as matrix cracking, delamination, fiber-matrix debonding and fiber breakage might appear during the manufacturing and service processes, among which delamination is the main form of destruction [4, 5]. Layered buckling is easy to occur in laminated composite plate structure at a low load level due to the existence of delamination, resulting in the expansion of

delamination as well as other damages and leading to the early occurrence of overall instability and failure of the structure. Moreover, FRP composite will be exposed to air, water, sunlight and other environments in processing, storage and application. Polymer is sensitive to these environmental factors and susceptible to aging due to the effects of these factors. Degradation will occur at the interface between matrix and fiber with the aging time extending, so that the natural aging of the composite also has a certain impact on its service. Therefore, the study on natural aging of FRP, delamination damage behavior and damage pattern recognition plays a significant role in structural health monitoring of the composite.

✉ Wei Zhou, zhouweihy@126.com; zhouwei@hbu.edu.cn; ✉ Lian-hua Ma, lhma@hbu.edu.cn | ¹College of Quality and Technical Supervision, Hebei University, Baoding 071002, China. ²National and Local Joint Engineering Research Center of Metrology Instrument and System, Baoding, China.



For FRP composite, the environmental conditions such as humidity, heat and light have obvious influence on its mechanical properties, which will lead to the decrease of its strength and stiffness as time passes by. Hence, the aging property of FRP is an essential part of structural health monitoring. In order to evaluate the correlation between natural aging and accelerated aging, the degradation of the mechanical and physical properties of graphite-epoxy composites exposed to natural environments and accelerated environmental conditions respectively was investigated by Shin et al. [6]. The results show that transverse flexural property of composite is sensitive to environmental damage, moreover, the strength and stiffness of the material after exposure decrease exponentially with the aging time. Furthermore, the mechanical properties of hybrid composite and glass fiber composite after accelerated environmental aging were evaluated by Rodrigues et al. [7]. The results indicate that there is a mechanical degradation in the aged material and hybrid composite is more sensitive to aging than glass fiber composite.

Because of the low interlaminar strength of composite laminates, interphase failure can be easily caused by interlaminar stress. Delamination damage easily occurs at the interior of the composite if the laminate is physically impacted in the process of assembly, repair and adaptation, which is not easy to find but with a high probability and can reduce the bearing capacity of the structure [8, 9]. In order to study the failure behavior of delamination, some scholars have done many researches. Zhou et al. [10] carried out three kinds of specimens to study the effects of delamination positions and lengths on compressive behavior of the composite. The results indicate that multi-delamination defects lead to the reduction of mechanical properties, and the lengths and positions of delaminations and the thickness of sub-layer have significant influence on buckling behaviors. The mixed-mode delamination failure properties of composite laminates in hygrothermal environment were investigated by Liu et al. [11]. The analysis of initial defect of delamination and different failure modes indicates that load mode and hygrothermal environment affect the delamination properties remarkably and the delamination shear resistance of unidirectional laminates is less than that of angle-plylaminates. Furthermore, the unity between computational predictions and experimental results in terms of the emergence and growth of delamination, growth stability, structural response and the maximum strains was certified by Wimmer et al. [12].

In the last decades, mechanical testing is generally used to study the failure characteristics of composite, most of which only provide information about final failure without damage evolutionary propagation. Acoustic emission (AE) technique as a non-destructive testing technology primarily

overcomes the limitation, which can monitor the damage and failure behaviors of composite in real-time and provide useful information for investigating the damage pattern recognition through cluster analysis [13, 14]. Based on AE signals, the combined method including k-means algorithm and k-nearest neighbor was used by Godin et al. [15] to investigate the progressive damage mode in glass/polyester composite under tensile loading. It is found that matrix creaking and interfacial decohesion are main damage modes, which indicates that this method has a good effect on the clustering results of AE signals from different mechanical sources. Furthermore, the delamination onset and propagation under quasi-static and fatigue loading were determined by Silversides et al. [16]. The results indicate that micro-damage mechanisms occurring before delamination can be detected by AE monitoring and AE signals can be related to delamination growth rate.

This paper investigates the comparative study of mechanical properties and AE response behavior of unidirectional glass and carbon-glass orthogonal woven fiber reinforced composites containing symmetric delaminations under three point bending testing. Moreover, the damage mechanisms of specimens are recognized by k-means clustering analysis. The effects of delaminations, reinforced materials and fiber orientation on buckling failure behaviors and the effects of natural aging on mechanical properties are discussed.

The organizational structure of this paper is as follows: firstly, the influence of delaminations on the buckling behavior of specimens under three-point bending load is studied in Sect. 3.1 by comparing and analyzing the damage evolutionary behavior of Specimen A and Specimen B. Next, based on the control variables, the effects of reinforced materials and fiber orientation on the buckling failure of specimens have been discussed in Sect. 3.2 through the comparative analysis of Specimen B with Specimen C and Specimen C with Specimen D respectively. Finally, in order to research the effects of natural aging on mechanical properties of specimens, the mechanical behaviors of two unidirectional glass fiber reinforced composites (with and without delaminations) exposed to natural environment is characterized in Sect. 3.3.

2 Experimental procedure

2.1 Materials and specimens

Four types of composite laminates were prepared with 12 layers fiber fabric, among which Specimen A and Specimen B contained 12 layers of unidirectional glass fiber (ECW 600–1270, 600 g/m²), specimen C and specimen D contained 8 layers of unidirectional glass

fiber and 4 layers of carbon-glass orthogonal woven fiber (placed on 2nd, 5th, 8th and 11th layers respectively). The lay-ups are $[0_G, (0_G/90_C), 0_{G2}, (0_G/90_C), 0_G]_5$ and $[0_G, (0_C/90_G), 0_{G2}, (0_C/90_G), 0_G]_5$ resulting in laminates of specimen C and D. A summarization of the characteristics of Specimen A, B, C and D is shown in Table 1. The composites were manufactured by vacuum assisted resin infusion (VARI) method. The mass ratio between epoxy resin (3329A) and curing agent (3329B) is 10:4. The as-prepared composites were cured for 48 h at room temperature and then solidified for 8 h at 130 °C. After cooling to room temperature, the prepared laminated plates with the thickness of 5 ± 0.2 mm were cut into specimens with the size of 140 mm \times 25 mm. Teflon films with the size of 30 mm \times 25 mm were sandwiched between 2 and 3th layers, 5th and 6th layers, 7th and 8th layers, 10th and 11th layers in Specimen B, C and D respectively to simulate the symmetric multiple delaminations. There is no delamination in Specimen A, but Specimens B, C and D have the same symmetrical multiple delaminations. Sketch map and fiber laying direction for four types of composite specimens are shown in Fig. 1 and Fig. 2 shows that Specimen B, C and D are divided into 5 daughterboards and substrate part by four delaminations, of which ①–⑤ are daughterboards and ⑥ is substrate.

2.2 Experimental equipment and process

Referring to ASTM D7264 standard, the three-point bending tests of the composite specimens were carried out at a crosshead speed of 2 mm/min by the LD24 machine. The span for three-point bending tests was 90 mm. At the same time, the AE real-time signals during the damage and evolution process were collected by using AE equipment (DS-2A). Two wideband sensors with frequency range of 100–900 kHz (VS900-RIC) were symmetrically distributed on both sides of the specimen with a center spacing of 90 mm. Experimental test system is shown in Fig. 3. In order to ensure good acoustic coupling, the lead-break test should be carried out before bending loading

test, and vacuum silicone grease should be fully applied between the sensors and the composite specimens. In order to effectively eliminate the electric and mechanical noise, the suitable threshold was fixed to 5 mV (34 dB) by repeated tests. The sampling frequency was 3 MHz. The peak definition time (PDT), hit definition time (HDT) and hit lock out time (HLT) were set to 30 μ s, 150 μ s and 300 μ s, respectively [17].

3 Results and discussions

3.1 Effects of delaminations on damage evolution of specimens

In order to understand the effects of delaminations on damage evolution of specimens, the mechanical performance curves of unidirectional glass fiber reinforced composite specimens with and without symmetric delaminations under three point bending testing are investigated. As shown in Fig. 4, the ultimate load of 3.47 kN is reached when the load of Specimen A increases at an approximately uniform rate to the point of instability failure. However, due to the existence of delaminations, Specimen B goes through I, II and III stages corresponding to the instability failure of daughterboard of ①, ② and ③ respectively. The ultimate strength of Specimen B is much less than that of Specimen A, indicating the degradation of carrying capacity of composite can be extremely influenced by the existence of delaminations, which is confirmed by Kazemianfar et al. [18]. According to the comparison of the two mechanical curves, the slope of Specimen A is higher than the overall slope of Specimen B. This outcome suggests that the defect of symmetrical multiple delaminations may result in a decrease in the stiffness of composite [19, 20]. Furthermore, the slope in stage I, II and III of Specimen B successively decreases with bending load increasing, which shows that the resistance to deformation when the structure is under stress becomes

Table 1 Comparison of characteristic parameters of Specimen A, B, C and D

	Reinforced materials and number of layers	Lay-ups	Existence of delaminations
Specimen A	12 layers of unidirectional glass fiber	$[0_G]_{12}$	No
Specimen B	12 layers of unidirectional glass fiber	$[0_G]_{12}$	Yes
Specimen C	8 layers of unidirectional glass fiber and 4 layers of carbon-glass orthogonal woven fiber	$[0_G, (0_G/90_C), 0_{G2}, (0_G/90_C), 0_G]_5$	Yes
Specimen D	8 layers of unidirectional glass fiber and 4 layers of carbon-glass orthogonal woven fiber	$[0_G, (0_C/90_G), 0_{G2}, (0_C/90_G), 0_G]_5$	Yes

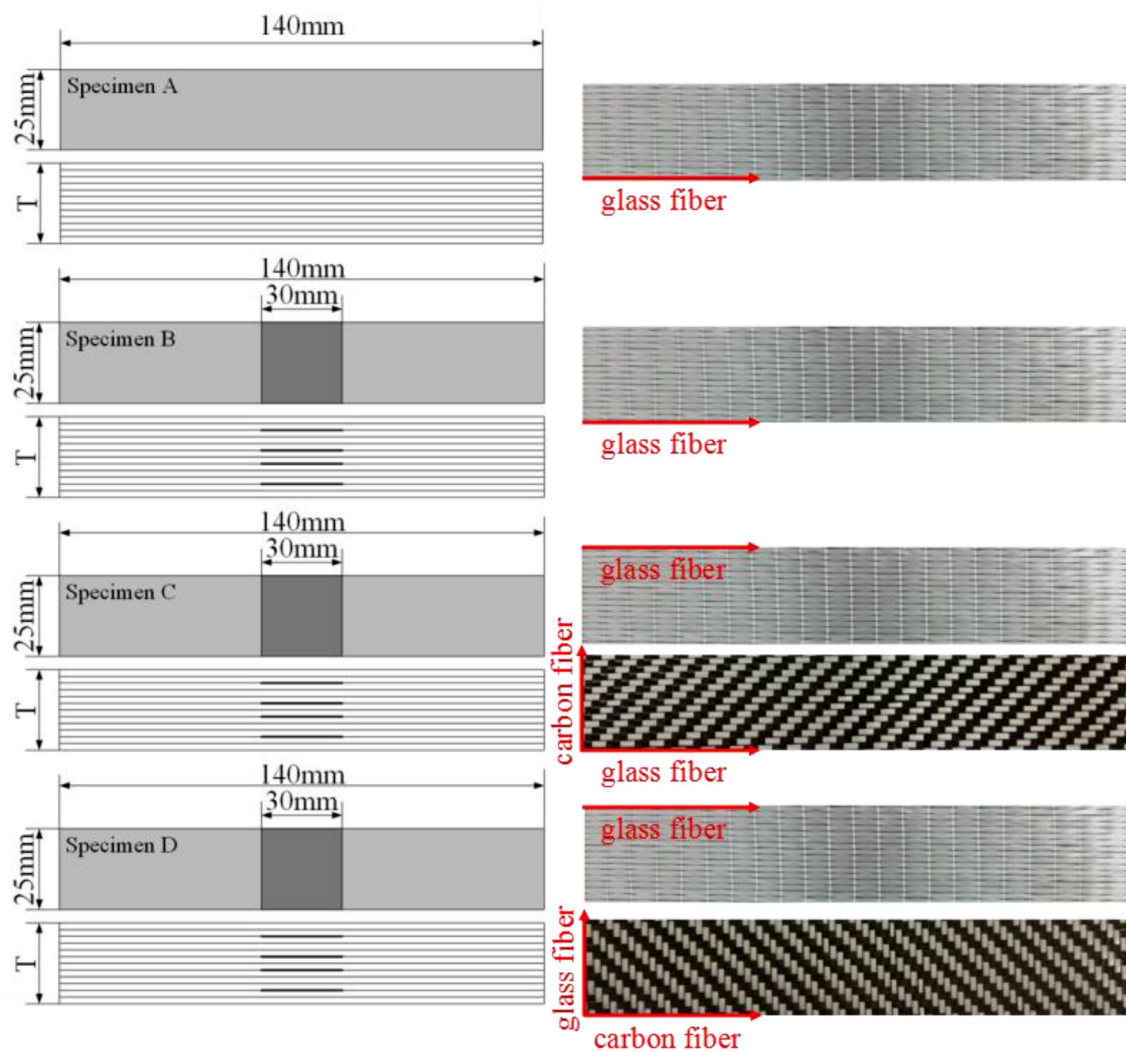


Fig. 1 Schematic diagram and fiber laying direction diagram for four types of composite specimens

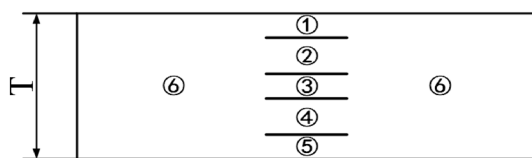


Fig. 2 Sketch map of specimen with symmetric multiple delaminations

increasingly weaker because of the instability failure of the previous daughterboard. It is generally known that three point bending loading makes the upper and lower sides of Specimen B bear pressure and tension respectively. Therefore, the sequential fractures of the daughterboard of ①, ② and ③ illustrate that delamination is more sensitive to pressure than tension [21, 22]. From a macro perspective, the catastrophic failure of specimen

without defects is explosive but the instability failure of specimen containing symmetrical multiple delaminations is intermittent.

In order to better reflect the AE response behavior and identify the damage evolution of Specimen B, the parameters of AE signal should be combined for analysis. The distribution characteristics of AE relative energy of Specimen A and B with the variation in time are shown in Fig. 5. Signals appearing in the first 50 s of loading might be noise signals, which may be caused by friction between specimens and loading system. It can be observed from Fig. 5a that for Specimen A, there are few damage signals during early- and medium-period of loading, but abundant high-energy damage signals occur in the later-period. This phenomenon indicates that the damage of Specimen A is concentrated in the point of buckling failure. This acoustic result is consistent

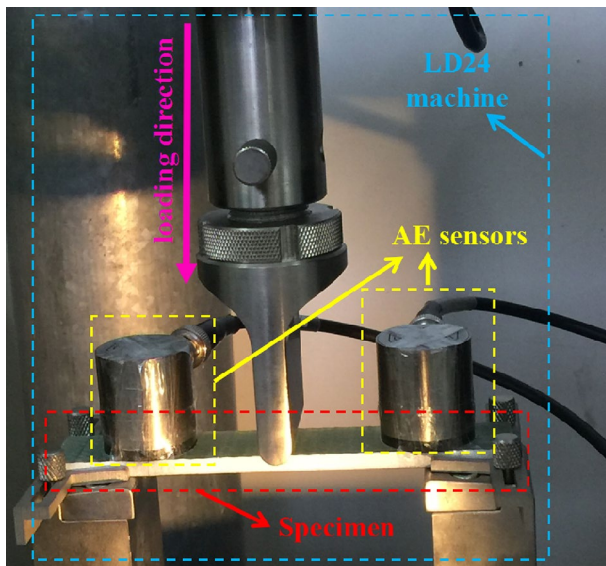


Fig. 3 Experimental test system of three point bending testing

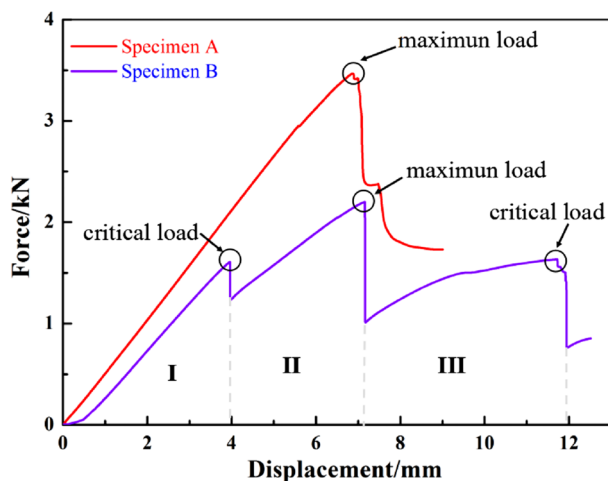


Fig. 4 Comparison of mechanical properties of Specimen A and B

with mechanical result: the catastrophic failure of Specimen A is explosive. Specimen B undergoes three energy-release stages, and high energy signals are concentrated at three critical failure points. The damage signals of stage I, II and III can be clearly observed from Fig. 5b. There are a few low-energy signals in stage I, and the quantity of signals in stage II increases, furthermore, the quantity and energy of signals in stage III increase obviously. The gradual damage indicates that with damage accumulating, the energy at each stage tends to increase until the instability fracture of daughterboard producing the highest energy signal at that stage. By comparing the energy and quantity of damage signals in each stage, the overall damage degree of Specimen B increases

gradually and the instability failure shows intermittent development.

For visualization, good classification results (see Fig. 6) are obtained by using k-means algorithm with three possible classes and the chosen features (amplitude, frequency and RA value (the ratio of rise time to amplitude)). The signals are divided into three clusters: low-frequency, medium-frequency and high-frequency, corresponding to matrix cracking, interphase failure and fiber breakage respectively [23, 24]. The cluster bounds of each damage mechanism and the number of AE events of Specimen A and B are shown in Table 2. It is clear that the amplitude distribution range of fiber breakage is lower than that of matrix cracking and interphase failure, which is consistent with the experimental result of Zhou et al. [25]. Combine Fig. 6 with Table 2, due to the low interlaminar strength of composite laminates, interphase failure is the main damage component in Specimen A and B. However, because of the existence of multiple delaminations, there are more interface failure signals in Specimen B than Specimen A. The cumulative hits of damage signals versus time is a good indication of damage evolution. As observed from Fig. 6, cumulative hits of Specimen A increases gently in early- and medium-period, but rapidly in later-period. As for Specimen B, cumulative hits continues to increase rapidly except for early-period. The cumulative hits-time curves of Specimen A and B are concave and convex respectively, indicating the damage degree of Specimen B is significantly severer in medium-period than that of Specimen A.

Based on the damage evolution process, the development of signal frequency over time of three damage mechanisms can be seen from Fig. 6. Some signals appearing in the first 50 s of loading might be related to external environment. It can be clearly observed that damage signals of Specimen A are concentrated in later-period, while damage signals of Specimen B are concentrated in middle- and later- loading period, which is consistent with cumulative hits growth trend. Matrix acting as a support first contacts and bears applied stress, however, the interphase structure of composite laminates is the most fragile. Therefore, damage signals of matrix cracking and interphase failure including fiber-matrix debonding and delamination expansion almost occur at the same time. It is well known that damage first develops in the direction of least resistance, so damage first appears in matrix and interphase. Subsequently, stress concentration promotes the propagation of cracks and delaminations. With the increase of load and bending deformation, fiber yarns gradually support the main load and the signals associated with fiber failure are gradually generated. Finally, buckling instability occurs and signal superposition results in the generation of a large number of high-energy damage

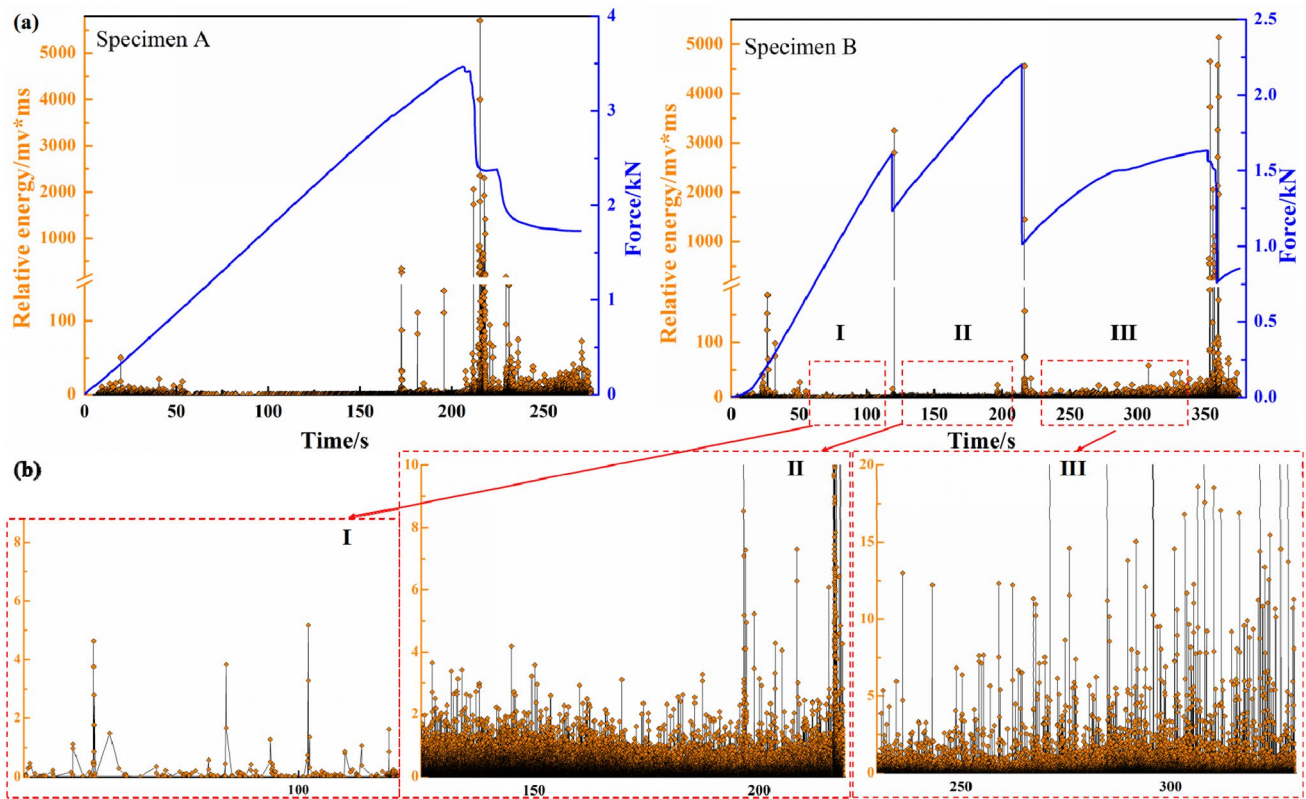


Fig. 5 The distribution characteristics of AE energy of Specimen A and B versus time

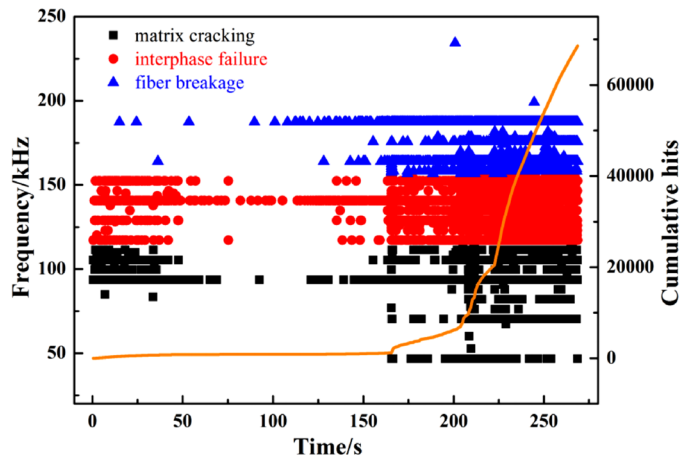
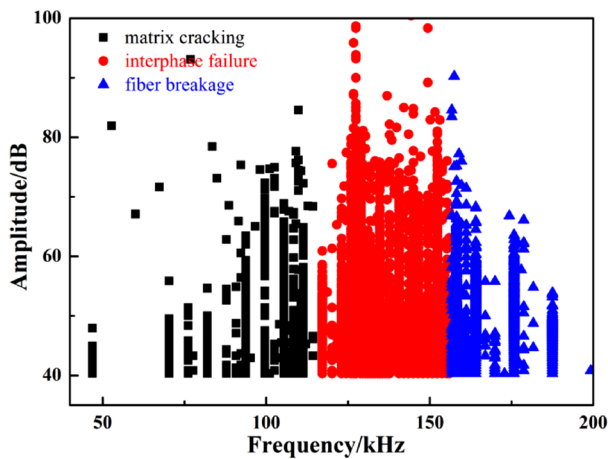
signals (see Fig. 5). The evolution process of three types of damage in Specimen A and B is similar, except that Specimen B undergoes three gradual processes. To sum up, the existence of symmetrical multiple delaminations will aggravate the damage of composite and make instability failure characterized by intermittency.

3.2 Effects of reinforced materials on the buckling failure of specimens

In order to determine the effects of reinforced materials and fiber orientation on the buckling failure of specimens, the mechanical properties of epoxy composite reinforced by unidirectional glass fiber and carbon-glass orthogonal woven fiber are investigated experimentally, as shown in Fig. 7. Based on the control variables, the independent variable between Specimen B and C is the reinforced material placed on 2nd, 5th, 8th and 11th layers and the independent variable between Specimen C and D is the layer orientation of carbon-glass orthogonal woven fiber. It is generally known that 90°-oriented unidirectional fiber basically does not bear stress under the action of three-point bending, while 0°-oriented unidirectional fiber bears the main load. For both Specimen B and Specimen C, although glass fiber is subjected to bear the applied load,

the carbon-glass woven fiber cloth is thicker than unidirectional fiberglass cloth resulting that Specimen C is slightly thicker than Specimen B and the energy absorption capacity of Specimen C is stronger than that of Specimen B. This well explains why the ultimate strength of Specimen C are greater than that of Specimen B, as shown in Fig. 7. The strength and stiffness of carbon fiber are higher than glass fiber [26]. Based on lay-ups, the glass fiber in Specimen C and the carbon fiber in Specimen D are subjected to bending load respectively. Hence, the ultimate strength of Specimen D is higher than that of Specimen C. However, the ultimate load of Specimen D is only slightly higher than that of C, the reason of which may be that there is an angle deviation in the laying direction of carbon-glass hybrid fiber bundle (the direction of carbon fiber is not completely perpendicular to the loading direction). As a parameter to characterize the stiffness of the material, the slope of the mechanical curve indicates that the resistance to deformation of specimen B and D is basically the same, which is higher than that of Specimen C. The cause of this phenomenon is as follows: due to the high flow resistance of the liquid resin in the hybrid woven fabric, the resin perfusion quality on hybrid woven fabric is lower than that on unidirectional fabric leading to the generation of more random void defects, which has influence on

(a) Specimen A



(b) Specimen B

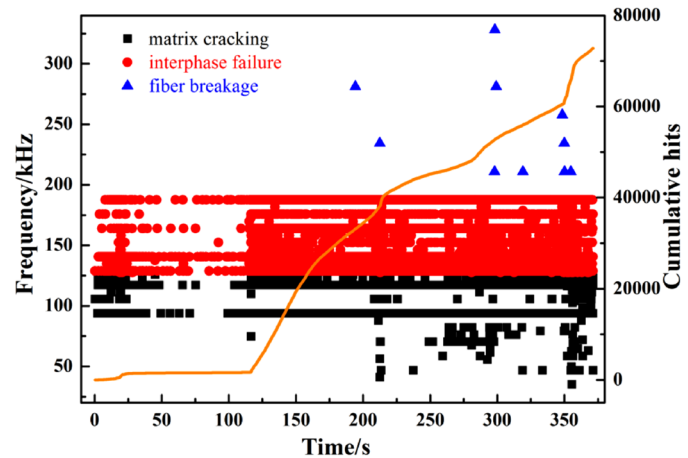
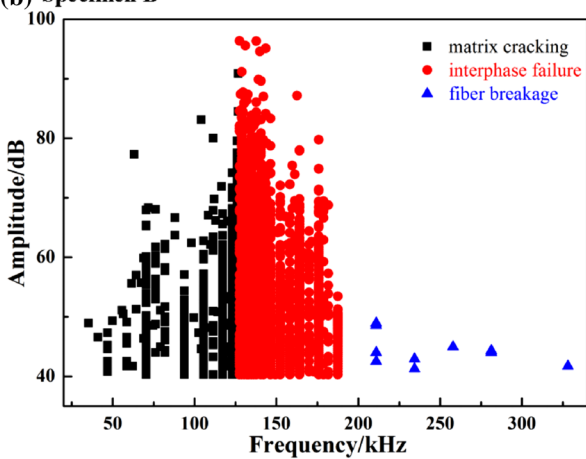


Fig. 6 Clustering results and cumulative hits of Specimen A and B

Table 2 Cluster bounds of each damage mechanism and the number of AE events of Specimen A and B

	Amplitude/dB	Frequency/kHz	Number
Specimen A			
Matrix cracking	40–93	47–114	5431
Interphase failure	40–100	117–156	51,509
Fiber breakage	40–90	156–235	11,640
Specimen B			
Matrix cracking	40–90	35–126	6826
Interphase failure	40–96	127–187	65,963
Fiber breakage	41–49	210–328	10

the mechanical properties [27, 28]. As shown in Table 3, the microphotography technology is used to calculate the void percentage of specimens. It can be observed that there are a small quantity of small voids in Specimen B, but more large voids in Specimen C and Specimen D. The void percentages of Specimen B, C and D are 1–3%, 5–7%

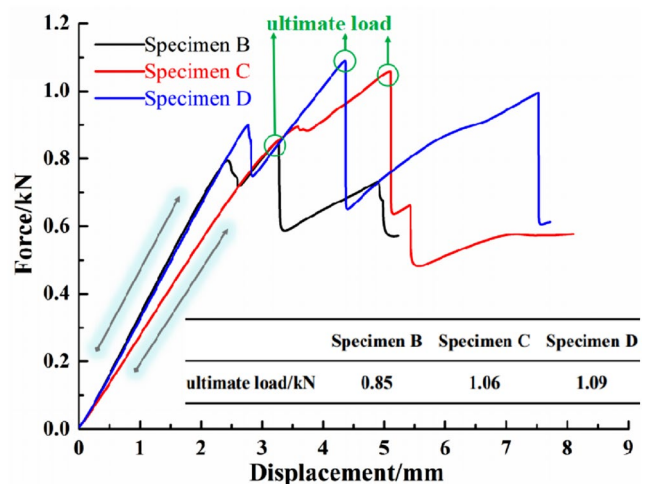
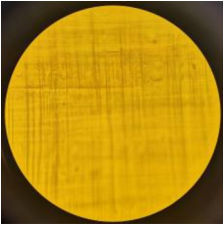
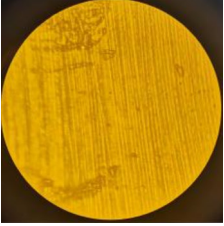
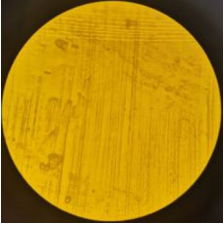


Fig. 7 Comparison of mechanical properties of Specimen B, Specimen C and Specimen D

Table 3 Calculation and characterization of porosity of Specimen B, C and D

Specimen	Microscopic image	Void percentage (%)
Specimen B		1–3
Specimen C		5–7
Specimen D		5–7

and 5–7%, respectively. Although the bearing structure of Specimen B and Specimen C is glass fiber, the greater porosity may be partly responsible for the smaller slope. As for Specimen D, the dual effects of the porosity and carbon fiber bearing load result in its slope is approximately the same as that of Specimen B. In conclusion, layer thickness, porosity and fiber orientation are important factors influencing the reliability of fiber reinforced composite plates.

With respect to acoustic results of Specimen B, C and D, the distribution characteristic of AE energy versus time is shown in Fig. 8. Because of the existence of symmetrical multiple delaminations, Specimen B, C and D experience three partial buckling failures, in addition, the overall instability failure is characterized by intermittency. The signal energy of Specimen B, C and D have a similar evolution: with the accumulation of damage, the quantity and energy of damage signals increase gradually until a large number of high-energy signals are generated when specimen is suffering from partial buckling failure. As for the clustering results of Specimen B, C and D, Fig. 9 indicates that there are three damage mechanisms in each specimen: matrix cracking, interphase failure and fiber breakage. It is clear that signals associated with fiber damage are characterized with the highest frequency and lowest amplitude.

The AE signals of Specimen B and Specimen C are clustered into three classes, the distribution of frequency and the number of signals in each class are shown in Figs. 9 and 10. As for Specimen B, the most AE signals about matrix cracking have a low frequency in the range of 0–50 kHz, the frequency of interphase failure is slight higher mainly in the range of 50–100 kHz, fiber breakage with the high frequency is centralized in the range of 150–200 kHz. In terms of Specimen C, the frequency of matrix cracking, interphase failure and fiber breakage are mainly in the range of 0–100 kHz, 100–150 kHz and 200–300 kHz. By comparison, the frequency range of each type of damage in Specimen C is wider than that of Specimen B. It is clear that the number of signals relating to interphase failure in specimen B is the largest, indicating interphase failure plays a leading role in damage evolution process of Specimen B due to the existence of symmetrical multiple delaminations. However, there are the most signals corresponding to matrix cracking in Specimen C. The main reason for this phenomenon is that the effect of porosity on matrix plays a leading role in the buckling failure process of specimen, and the effect of delamination defects on mechanical properties plays a secondary role [27, 28]. This again confirms that the porosity of hybrid woven fabric is higher than that of unidirectional fabrics. Compared with Specimen C, there is more severe interphase failure in Specimen D, which may have a relationship with damage behavior of carbon fiber.

3.3 Effects of natural aging on mechanical properties of specimens

The essence of aging is a change in its physical or chemical structure, that is any destructive reaction caused by physical, chemical or mechanical factors (i.e. degradation), causing the progressive deterioration of composite properties [29, 30]. In order to evaluate the property degradation of composite in storage, the mechanical behaviour of two unidirectional glass fiber reinforced composites (with and without delaminations) exposed to natural environment is characterized. The specimens are naturally placed indoors to simulate storage condition. The experimental parameters of natural aging are shown in Table 4.

As shown in Fig. 11 and Table 5, the ultimate loads of unaged Specimen A and B and aged Specimen A and B are 3.52 kN, 2.2 kN, 2.72 kN and 0.85 kN respectively. It can be seen that the ultimate strength of the aged Specimen A and B is 77.27% and 38.64% of the original Specimen A and B, respectively. The ultimate strength of the aged specimen containing delaminations decreases more obviously, indicating that the delamination defect is more sensitive to the aging condition. The reason for this phenomenon is as follows: light, heat, humidity, oxygen and

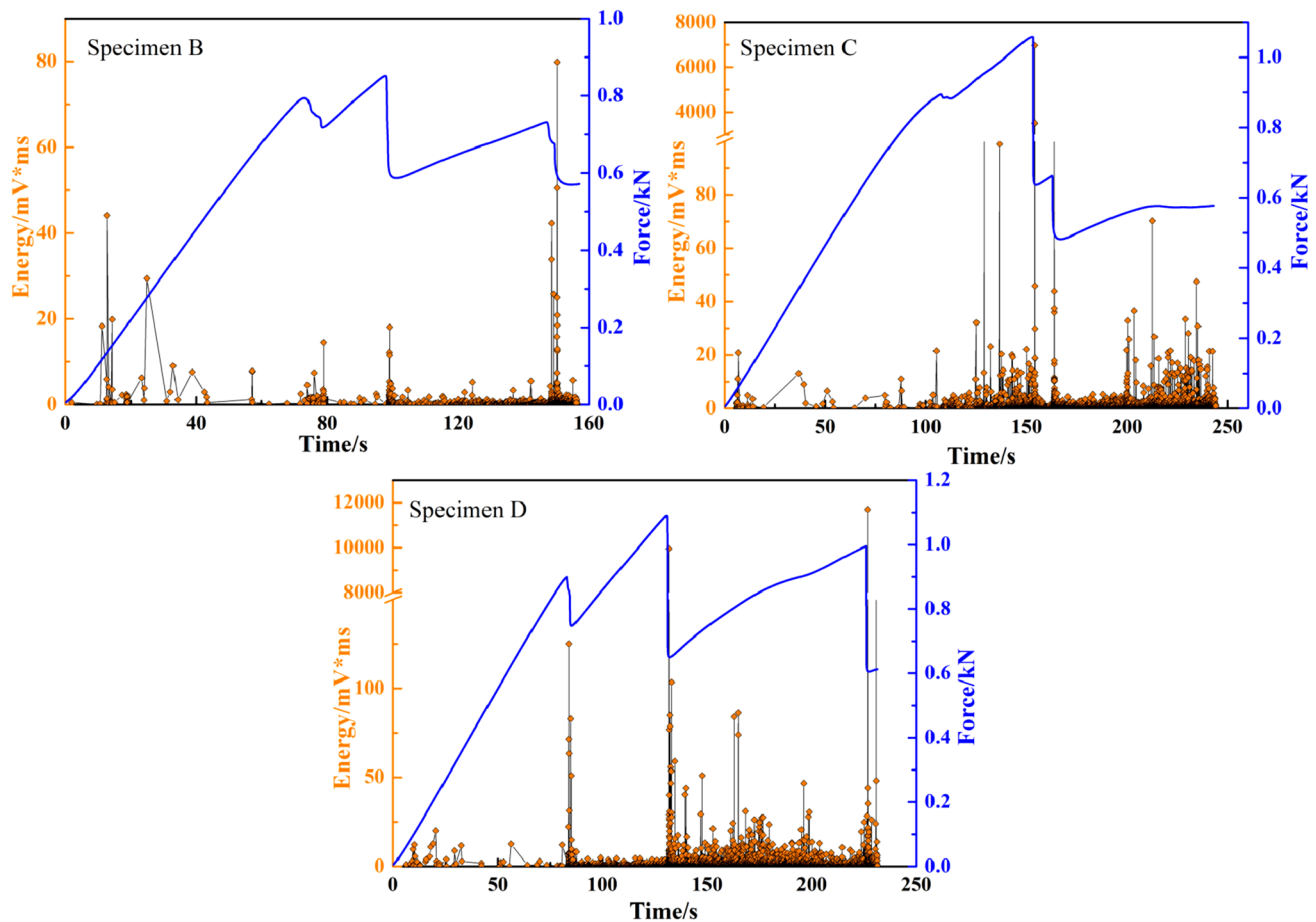


Fig. 8 The distribution characteristics of AE energy of Specimen B, C and D versus time

other factors and the change of polymer composition and state structure are the main external and internal factors causing the aging of materials [31]. During degradation, the first barrier to receive external factors is the matrix and the ultraviolet light from natural light can cause partial degradation of macromolecular chains in the resin matrix, so that the mechanical properties of the composite material can be significantly reduced after aging [32]. However, the surface morphology of the specimen is basically unchanged as the natural aging time is short. Furthermore, the water in air can lead to internal stress in the specimens due to the plasticization and swelling of the matrix and the expansion mismatch between resin and fiber [33], which will easily result in the expansion and degradation of the delamination. Therefore, the main reason why the delamination defect is more sensitive to aging is that water diffuses into the specimen resulting in further weakening of the delamination interface. In addition, it can be seen from Fig. 11 that the slope of the mechanical curves of the aged specimens decreases compared with the original specimens, indicating that the aging condition will have a certain influence on the stiffness of the material, and make

the resistance to deformation of the material weakened, which was proved by Gruneberger et al. [34].

As a physical quantity, deflection can evaluate the physical properties of materials and reflect the toughness characteristic of materials. It refers to the linear displacement of specimen axis in the direction perpendicular to the axis. The experimental results show that the deflections of original Specimen A and B and aged Specimen A and B are 7.65 mm, 12.52 mm, 8.30 mm and 5.23 mm. Compared to original Specimen A, the deflection of the aged Specimen A increased slightly, which indicates that the natural aging process has a negative effect on the strength and stiffness of material, but may have a positive effect on the toughness of material. The reason why positive effect plays a leading role in terms of the toughness of Specimen A is that during a short aging period, the thermal stress generated in the curing process of the composite is gradually released by the stress relaxation of the resin matrix, consequently, the ability of material to absorb energy during plastic deformation and fracture can be improved. However, due to the existence of delaminations, the negative effect has more influence on the toughness of Specimen B

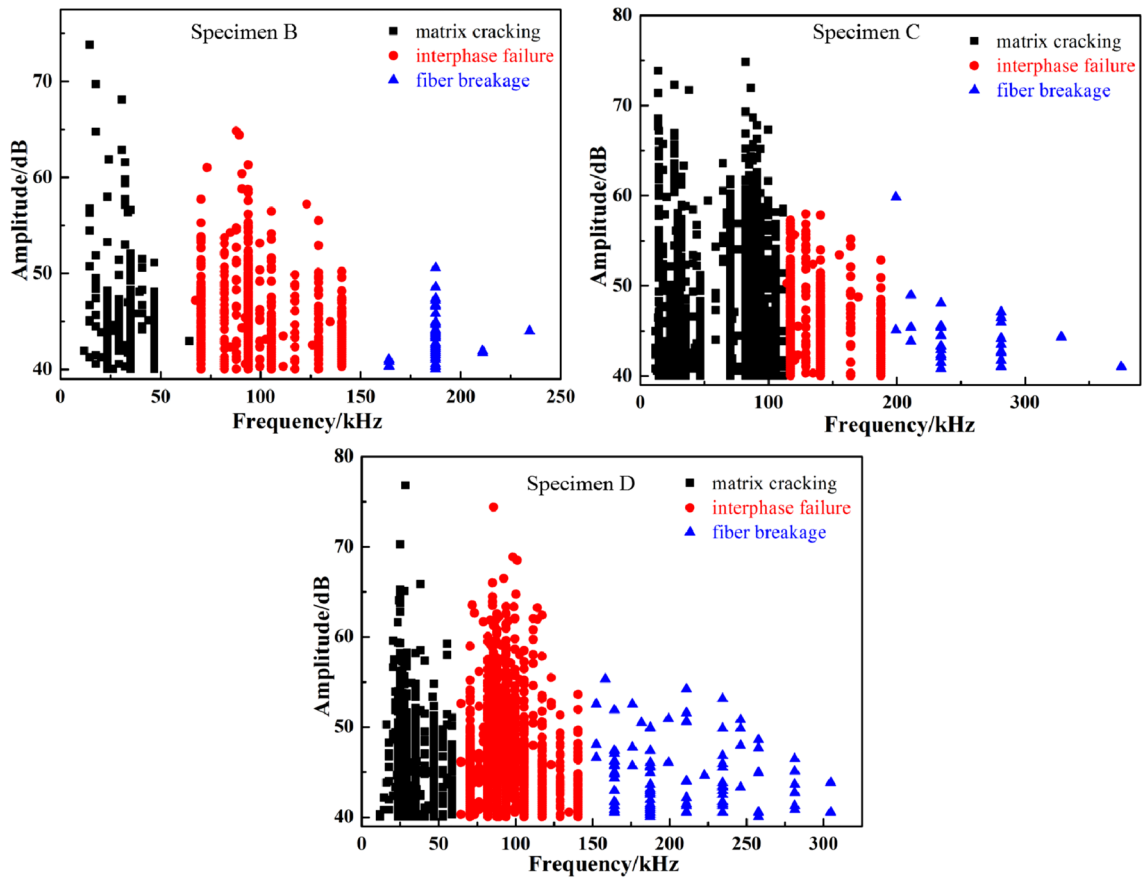


Fig. 9 Clustering results of amplitude and frequency of Specimen B, C and D

than the positive effect. Degradation of surface resin and weakening of interfacial properties play a leading role in aged Specimen B, so the deflection decreases significantly.

Combine with the AE cluster results in Sects. 3.2 and 3.3, the SEM analysis for original Specimen B and aged Specimen B is carried out to verify matrix cracking, interphase failure and fiber breakage, as shown in Fig. 12. The mechanical results show that the strength degradation due to natural aging of the specimens with delaminations is more obvious. Compared with original specimen, it can be seen that the interphase damage of aged specimen is more severe. There is only a small amount of single fiber debonding in original specimen, but large areas of interface debonding can be easily observed in aged specimen. Furthermore, failure morphology about matrix damage indicates that a large number of matrix fragments are attached to the periphery of fiber fracture in original specimen. In contrast, there almost no matrix fragments is found in the aged specimen. Through comparative analysis, it can be observed that the degree of matrix breakage of the aged specimen with a greater particle density of matrix fragments is greater than that of the original specimen. These results suggest that natural aging will not only

weaken the resin matrix, but also reduce the interfacial adhesion between the matrix and fiber, which has a great influence on the strength degradation of composite.

4 Conclusion

Three point bending tests are carried out with the aim of determining the effects of symmetric multiple delaminations, reinforced materials and fiber orientation on damage evolutionary behaviors and the effects of natural aging on mechanical properties of unidirectional glass and carbon-glass orthogonal woven fiber reinforced composites. The experimental results show that the degradation of carrying capacity and the resistance to deformation of composite can be extremely influenced by the existence of delaminations, which leads to the early occurrence of overall instability of the structure. In addition, the instability failure of the specimens containing symmetrical multiple delaminations is intermittent. The AE cluster analysis results indicate that matrix cracking, interphase failure and fiber breakage are characterized with the lowest, medium and highest frequency

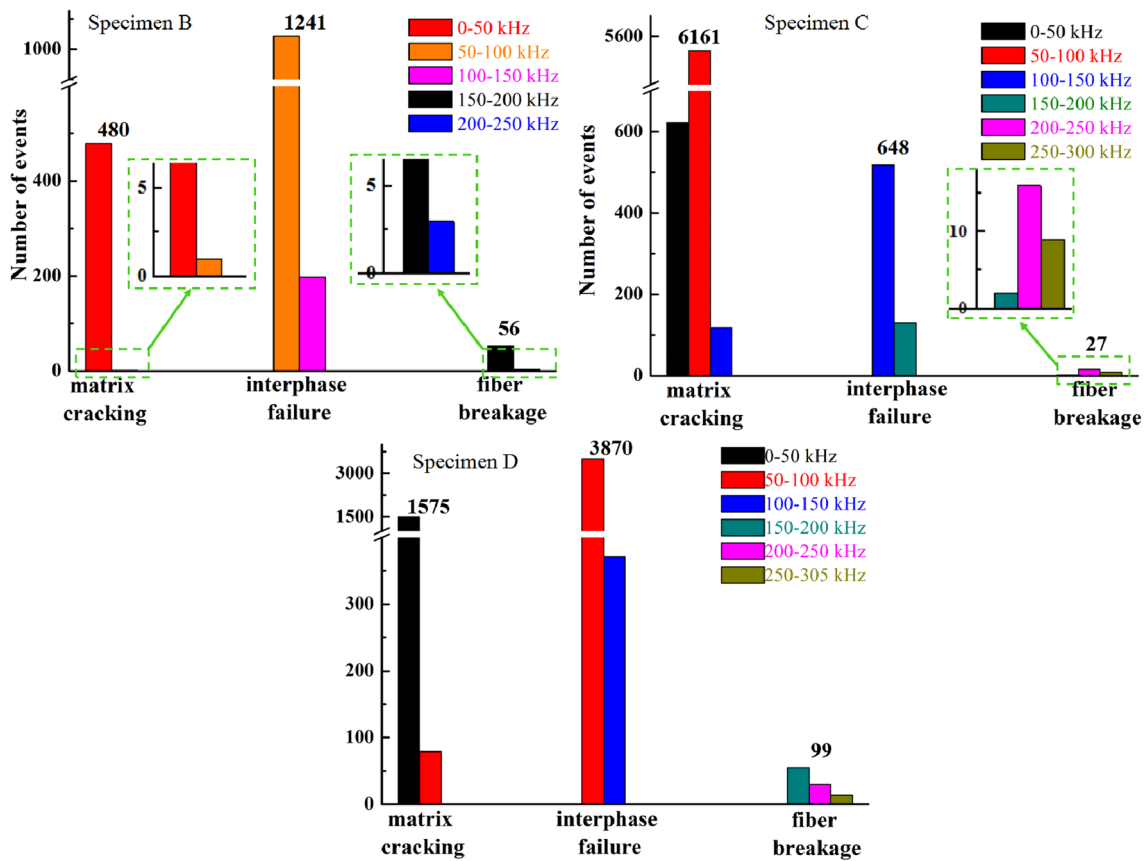


Fig. 10 Distribution of frequency and number of AE events of Specimen B, C and D

Table 4 The experimental parameters of natural aging

Ageing method	Ageing duration	Temperature	Relative humidity	Lighting condition
Naturally placed indoors	Eleven months	20–25 °C	40–50%	No direct sunlight

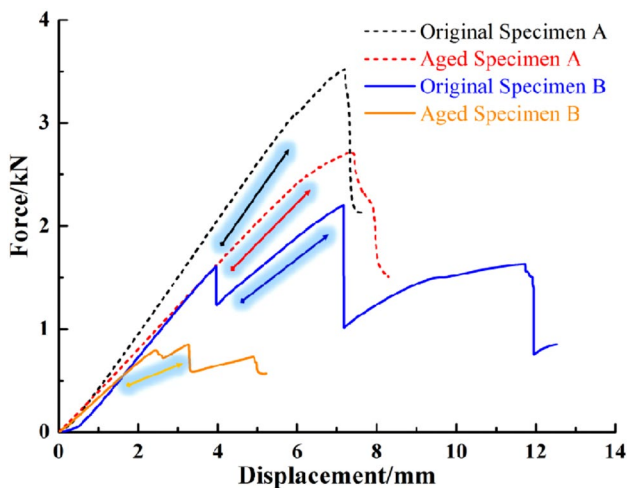


Fig. 11 Comparison of mechanical properties of original and aged unidirectional glass fiber reinforced composites

Table 5 Comparison of mechanical experimental results of aged and unaged specimens

Specimen	Original Specimen A	Aged Specimen A	Original Specimen B	Aged Specimen B
Ultimate load/kN	3.52	2.72	2.20	0.85
Deflection/mm	7.65	8.30	12.52	5.23

respectively. Furthermore, signals associated with fiber damage are characterized with the lowest amplitude. In addition, the differences of reinforced materials, layer thickness, porosity and fiber orientation are important factors influencing the reliability of composite laminates. Otherwise, the effects of natural aging on mechanical properties indicate that natural aging will reduce the strength and stiffness of the material but improve the toughness to a certain extent. Furthermore, the

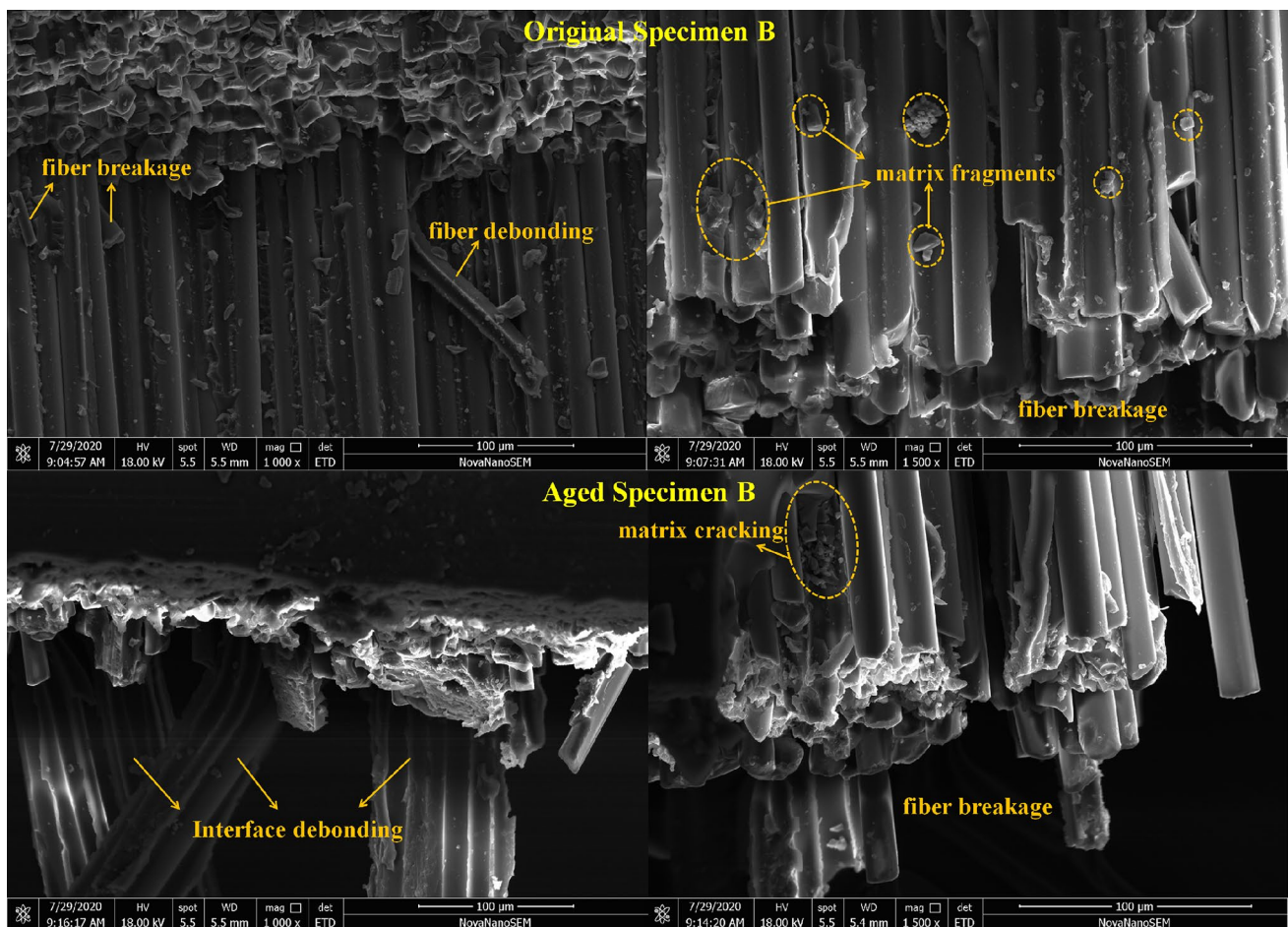


Fig. 12 The SEM analysis about failure morphology of original Specimen B and aged Specimen B

existence of delaminations makes the composite more sensitive to natural aging conditions.

Many uncertain factors in the process of processing and transportation and low energy impact in the process of assembly and service are most likely to lead to delamination defects, which have great limitations on the application of materials. In addition, the choices of reinforced materials and their orientation also have important influence on the performance of composite. Combine with test measurement, this paper has an important reference value for evaluating the comprehensive performance of composite laminates. However, in order to further evaluate the quality of composite, study the effect of delamination on service property of composite laminates and realize the visualization of failure morphology, combining with the common load conditions of composite, a more comprehensive experimental scheme needs to be proposed and more advanced detection methods need to be applied in future research to provides reference value for the structural health monitoring and engineering application of materials.

Acknowledgements The authors gratefully acknowledge the financial support of the National Natural Science Foundation of China (Grant No. 11502064 and 11572109).

Compliance with ethical standards

Conflict of interest The authors declare that they have no conflict of interest.

References

1. Vorathin E, Hafizi ZM, Ghani SAC et al (2018) FBGs real-time impact damage monitoring system of GFRP beam based on CC-LSL algorithm. *Int J Struct Stab Dyn* 18(5):1850075
2. Mouhmid B, Imad A, Benseddiq N et al (2006) A study of the mechanical behaviour of a glass fibre reinforced polyamide 6, 6: experimental investigation. *Polym Test* 25(4):544–552
3. Isitman NA, Aykol M, Kaynak C (2012) Interactions at fiber/matrix interface in short fiber reinforced amorphous thermoplastic composites modified with micro- and nano-fillers. *J Mater Sci* 47(2):702–710

4. Liu P, Groves RM, Benedictus R (2014) 3D monitoring of delamination growth in a wind turbine blade composite using optical coherence tomography. *NDT E Int* 64:52–58
5. Li L, Yan X (2018) Progressive damage analysis for cross-ply graded PE/PE composites based on cluster analysis of acoustic emission signals. *J Thermoplast Compos Mater* 31(5):634–656
6. Shin KB, Kim CG, Hong CS (2003) Correlation of accelerated aging test to natural aging test on graphite-epoxy composite materials. *J Reinf Plast Compos* 22(9):849–861
7. Rodrigues LPS, Silva RV, Aquino EMF (2012) Effect of accelerated environmental aging on mechanical behavior of curaua/glass hybrid composite. *J Compos Mater* 46(17):2055–2064
8. Xu D, Liu PF, Chen ZP et al (2019) Delamination analysis of carbon fiber/epoxy composite laminates under different loading rates using acoustic emission. *J Fail Anal Prev* 19(4):1034–1042
9. Szekrenyes A (2012) Interlaminar stresses and energy release rates in delaminated orthotropic composite plates. *Int J Solids Struct* 49(18):2460–2470
10. Zhou W, Lv ZH, Li ZY et al (2016) Acoustic emission response and micro-deformation behavior for compressive buckling failure of multi-delaminated composites. *J Strain Anal Eng Des* 51(6):397–407
11. Liu PF, Yang J, Peng XQ (2017) Delamination analysis of carbon fiber composites under hygrothermal environment using acoustic emission. *J Compos Mater* 51(11):1557–1571
12. Wimmer G, Kitzmueller W, Pinter G et al (2009) Computational and experimental investigation of delamination in L-shaped laminated composite components. *Eng Fract Mech* 76(18):2810–2820
13. Alia A, Fantozzi G, Godin N et al (2019) Mechanical behaviour of jute fibre-reinforced polyester composite: characterization of damage mechanisms using acoustic emission and microstructural observations. *J Compos Mater* 53(24):3377–3394
14. Godin N, Reynaud P, Fantozzi G (2008) Challenges and limitations in the identification of acoustic emission signature of damage mechanisms in composites materials. *Appl Sci Basel*. <https://doi.org/10.3390/app8081267>
15. Godin N, Huguet S, Gaertner R et al (2004) Clustering of acoustic emission signals collected during tensile tests on unidirectional glass/polyester composite using supervised and unsupervised classifiers. *NDT E Int* 37(4):253–264
16. Silversides I, Maslouhi A, LaPlante G (2013) Acoustic emission monitoring of interlaminar delamination onset in carbon fibre composites. *Struct Health Monit* 12(2):126–140
17. Kumar CS, Arumugam V, Santulli C (2017) Characterization of indentation damage resistance of hybrid composite laminates using acoustic emission monitoring. *Compos Part B Eng* 111:165–178
18. Kazemianfar B, Esmaeeli M, Nami MR (2020) Experimental investigation on response and failure modes of 2D and 3D woven composites under low velocity impact. *J Mater Sci* 55(3):1069–1091
19. Liu Z, Xia Y, Guo S (2019) Characterization methods of delamination in a plain woven CFRP composite. *J Mater Sci* 54(20):13157–13174
20. Juhasz Z, Szekrenyes A (2017) The effect of delamination on the critical buckling force of composite plates: experiment and simulation. *Compos Struct* 168:456–464
21. Lin MC, Lou CW, Lin JY et al (2018) Tensile strength, peel load, and static puncture resistance of laminated composites reinforced with nonwoven fabric. *J Mater Sci* 53(17):12145–12156
22. Szekrenyes A (2019) Analytical solution of some delamination scenarios in thick structural sandwich plates. *J Sandw Struct Mater* 21(4):1271–1315
23. Kempf M, Skrabala O, Altstadt V (2014) Acoustic emission analysis for characterisation of damage mechanisms in fibre reinforced thermosetting polyurethane and epoxy. *Compos Part B Eng* 56:477–483
24. Zhang PF, Zhou W, Yin HF et al (2019) Progressive damage analysis of three-dimensional braided composites under flexural load by micro-CT and acoustic emission. *Compos Struct* 226:111196
25. Zhou W, Zhao WZ, Zhang YN et al (2018) Cluster analysis of acoustic emission signals and deformation measurement for delaminated glass fiber epoxy composites. *Compos Struct* 195:349–358
26. Ramirez FA, Carlsson LA, Acha BA (2008) Evaluation of water degradation of vinylester and epoxy matrix composites by single fiber and composite tests. *J Mater Sci* 43(15):5230–5242
27. Mehdikhani M, Nguyen NQ, Straumit I et al (2018) Analysis of void morphology in composite laminates using micro-computed tomography. In: 13th International conference on textile composites 406: 012010
28. Kuentzer N, Simacek P, Advani SG et al (2007) Correlation of void distribution to VARTM manufacturing techniques. *Compos Part A Appl Sci Manuf* 38(3):802–813
29. Du Q, Zhang SJ, Pan BC et al (2014) Effect of spatial distribution and aging of ZVI on the reactivity of resin-ZVI composites for arsenite removal. *J Mater Sci* 49(20):7073–7079
30. Zhao M, Wu GH, Jiang LT (2004) Aging behavior and precipitation kinetics of SiCp/6061Al composites. *J Mater Sci* 39(5):1759–1763
31. Yang YQ, Ota T, Morii T et al (2011) Mechanical property and hydrothermal aging of injection molded jute/polypropylene composites. *J Mater Sci* 46(8):2678–2684
32. Shettar M, Kini UA, Sharma S et al (2020) Hygrothermal chamber aging effect on mechanical behavior and morphology of glass fiber-epoxy-nanoclay composites. *Mater Res Express* 7(1):015318
33. Garg M, Sharma S, Mehta R (2016) Carbon nanotube-reinforced glass fiber epoxy composite laminates exposed to hygrothermal conditioning. *J Mater Sci* 51(18):8562–8578
34. Gruneberger F, Kunniger T, Zimmermann T et al (2014) Nanofibrillated cellulose in wood coatings: mechanical properties of free composite films. *J Mater Sci* 49(18):6437–6448

Publisher's Note Springer Nature remains neutral with regard to jurisdictional claims in published maps and institutional affiliations.